CRYSTAL GROWTH & DESIGN

Article

pubs.acs.org/crystal

Rehabilitation of MgO(001) Substrate Surface for Growth of Single-Crystal $LaBaCo_2O_{5+\delta}$ Films by Magnetron Sputtering

Q. Y. Zhang,*[,†] J. Shaibo,[†] J. Ju,[†] M. Liu,[‡] S. Cheng,[‡] Y. J. Ma,[†] J. Y. Xiao,[†] X. N. Jiang,[†] and C. Y. Ma[†]

[†]Key Laboratory of Materials Modification by Laser, Ion and Electron Beams, and School of Physics and Optoelectronic Technology, Dalian University of Technology, Dalian 116024, China

[‡]Electronic Materials Research Laboratory, Key Laboratory of the Ministry of Education & International Center for Dielectric Research, Xi'an Jiaotong University, Xi'an 710049, China

Supporting Information

ABSTRACT: Single-crystal films are at the foundation of a number of advanced technologies, such as for devices related to microelectronics, optoelectronics, spintronics, and superconducting electronics. In this study, high-temperature annealing was used to rehabilitate the MgO(001) surface to improve the crystallinity of highly epitaxial $LaBaCo_2O_{5+\delta}$ (LBCO) films, which have demonstrated potential for applications in fast gas sensors. In comparison with the LBCO film grown on the as-received substrate, solid evidence is presented to support that the rehabbed substrates facilitate deposition of single-crystal LBCO films by radio frequency magnetron sputtering at the optimized conditions. Thus, substrate annealing is demonstrated to be a practical and effective method for rehabbing the damaged surface of a substrate induced by manufacture and surface milling and is promising for a range of important applications based on the growth of single-crystal films.

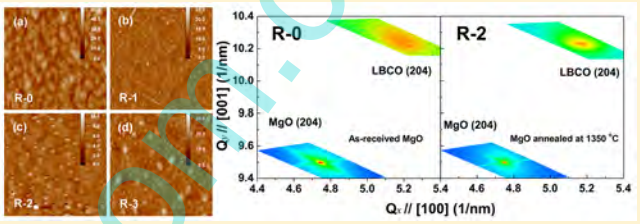

1. INTRODUCTION

$La_{0.5}Ba_{0.5}CoO_3$ (LBCO) is one of the most important cobalt-based perovskites among the strongly correlated electron oxides, exhibiting three perovskite-based forms, namely, the ordered, disordered, and nano-ordered structures.[1] LBCO has been found to have unusual physical properties. For instance, the ordered LBCO with space group $P4/mmm$ is semiconducting, but the other two phases with space group $Pm\bar{3}m$, corresponding to La and Ba disordering and nanometer-scale ordering, respectively, are semi-metallic conducting.[1] LBCO has been considered as the leading material for replacing standard metal electrodes as a cathode of solid oxide fuel cells.[2−5] On the other hand, LBCO has potential for applications in surface catalysts and chemical sensors. Recently, highly epitaxial LBCO films were successfully deposited on various substrates with cubic lattices, including MgO, $LaAlO_3$, $SrTiO_3$ (STO), and $NdGaO_3$, using the pulsed laser deposition (PLD) method.[6−14] The LBCO films were suggested to have the ordered phase with oxygen deficiency ($LaBaCo_2O_{5+\delta}$)[6,7] but exhibited physical properties rather different from their bulk materials. The as-grown LBCO films on (001) MgO substrates were found to have large magnetoresistances as large as 54% at 40 K under 7 T.[7] In addition, an anomalous magnetic hysteresis, depending strongly on temperature and applied magnetic field scan width, was reported.[7] More importantly, the LBCO films could quickly respond to the ambient gas in a few seconds at relatively low temperatures. A reproducible resistance response of over 99% was achieved in the LBCO film during a change from 4% H_2 and 96% N_2 to oxygen at a temperature range of 400−780 °C;[12] thus, highly sensitive gas sensors operating in reducing/oxidizing environments were demonstrated.[13,14] For the purpose of more cost-effective and large-scale applications, we explored the optimized parameters for deposition of highly epitaxial LBCO films using magnetron sputtering methods.[15]

It is well-known that substrate plays a crucial role in the growth of single-crystal films, which involves a number of advanced technologies related to microelectronics, optoelectronics, spintronics, and superconducting electronics. To obtain high-quality epitaxial films, lattice-matched substrates are preferred. In addition, a strict cleaning process is needed. For the growth of epitaxial LBCO films, (001) MgO is usually used as the substrate because its mismatch for the LBCO lattice is as small as ∼7%. However, MgO is too soft to be easily damaged during manufacture and surface milling. Therefore, the substrate surface contains a large amount of scratches, and there is a high density of defects such as point defects, dislocations, and stacking faults in the damaged layer beneath the substrate surface. Because the LBCO films are usually deposited at a relatively low temperature, these defects may not be removed before the film nucleation and may thus influence the crystallinity of the LBCO epilayers. As a matter of fact, surface damage is ubiquitous in substrate manufacture, but there are few articles investigating the influence of surface

Received: February 23, 2016
Revised: April 30, 2016
Published: June 28, 2016

DOI: 10.1021/acs.cgd.6b00308
Cryst. Growth Des. 2016, 16, 4272−4277

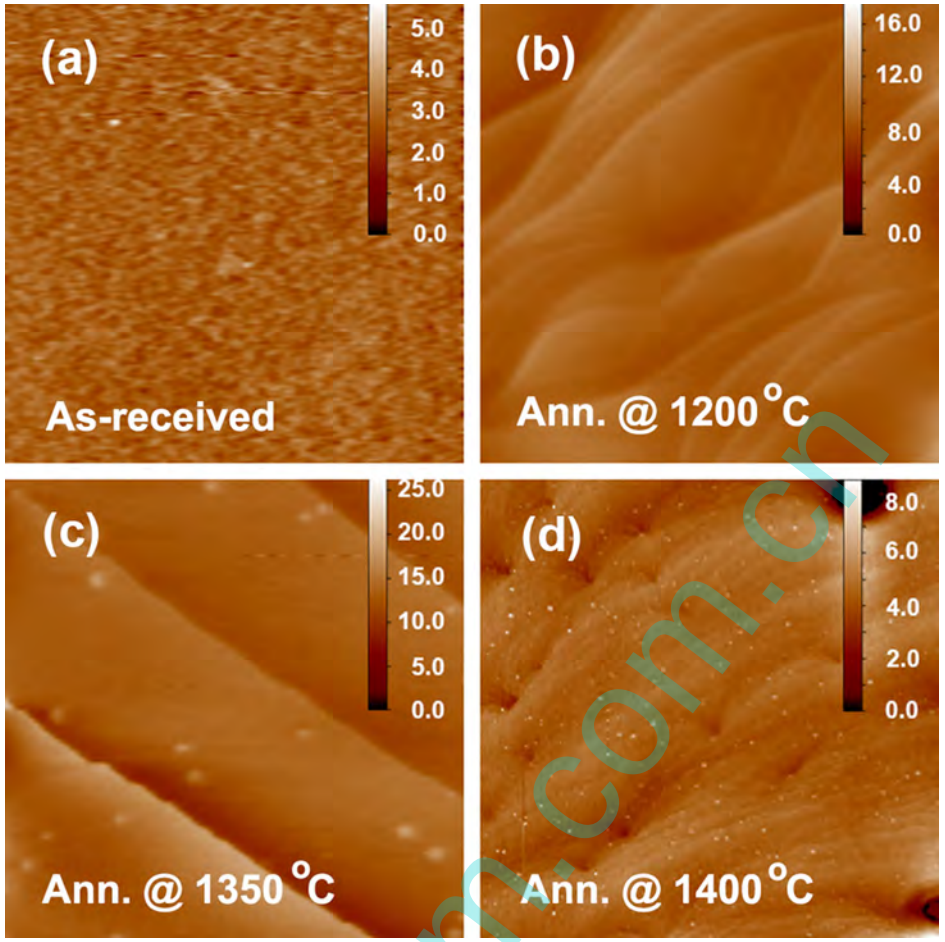

Figure 1. AFM images (4 × 4 μm) of (a) the as-received substrate and (b–d) substrates annealed at temperatures of 1200, 1350, and 1400 °C, respectively. The color rules are in nanometers to represent the variation in height.

damage on the crystallinity of epitaxial films or how to rehabilitate the damaged surfaces. In this article, we report our attempt to rehabilitate the damaged surface of the (001) MgO substrate using a high-temperature annealing method. With the consideration that the melting point of MgO is as high as ~2850 °C, an annealing process for rehabbing the damaged surface was conducted at temperatures close to half of its melting point, and then the rehabbed substrates were used to improve the crystallinity of epitaxial LBCO films deposited by the radio frequency (RF) magnetron sputtering method.

2. EXPERIMENTAL DETAILS

Epi-polished 5 × 10 mm (001) MgO substrates were used for the growth of epitaxial LBCO films. With the consideration that half of the melting point of MgO is ~1300 °C, the rehabilitation of the substrate surface by annealing was carried out in air at 1200, 1350, and 1400 °C. The MgO substrates, together with their ceramic containers, were annealed for 3 h in a muffle furnace. Before annealing, the substrates were strictly cleaned using a standard process. The LBCO films were deposited at an optimized temperature of 830 °C by RF magnetron sputtering of a 5 mm thick LBCO ceramic target in a diameter of 60 mm. As the crystallinity of a film depends on its thickness, all films for comparison were deposited under the same conditions, which lead to similar film thicknesses. The LBCO ceramic target was prepared by a solid reaction method in a manner similar to Millange et al.'s description.[16] For convenience in description, the LBCO film on the as-received substrate is labeled as R-0, and the films grown on the rehabbed substrates annealed at 1200, 1350, and 1400 °C are named R-1, R-2, and R-3, respectively. Prior to deposition, the vacuum chamber was pumped to a base pressure of ~2.0 × 10^{-4} Pa. Subsequently, a gas mixture of Ar and O_2 (6:60) was introduced for deposition of the LBCO films at a working pressure of ~4.5 Pa. The RF power applied to the LBCO target was 80 W. The ceramic target was presputtered for 15 min to avoid any contamination that may influence the nucleation and growth of the LBCO films. The LBCO films were characterized by X-ray diffraction (XRD, Bruker D8) and high-resolution XRD (Panalytical X'Per MRD). Contact-mode atomic force microscopy (AFM, Benyuan SPM 5000) was used to examine the surface morphology of the substrates and LBCO films. The chemical compositions of the LBCO films were analyzed using Auger electron spectroscopy (AES) and energy dispersive X-ray spectroscopy (EDX).

3. RESULTS AND DISCUSSION

High-temperature annealing can remove the scratches on the substrate surface and the lattice defects beneath the surface because the defects in the damaged layer move toward the surface and then vanish at the surface; thus, the substrate lattices are rehabbed to be higher quality and facilitate the epitaxial growth of films. However, annealing treatment cannot remove involatile contaminations on the substrate surface; thus, a strict cleaning process is crucial for rehabbing the substrate surface before annealing. More importantly, the rehabilitation must be conducted in a clean ambient environment to prevent pollution during the annealing process.

At a given temperature, evolution of vicinal surfaces of crystalline solids is thermodynamically driven by the density of

DOI: 10.1021/acs.cgd.6b00308
Cryst. Growth Des. 2016, 16, 4272–4277

the surface free energy (f), which depends on disorientation relative to the main crystallographic directions. For a single-crystal substrate, the density of the surface free energy is related to the miscutting angle (θ) and the miscut orientation (azimuth angle φ in respect to the angle with minimum f) through the following equation:[17]

$$f(\theta, \phi) = f_0 + \frac{\beta(\varphi)}{h}\tan\theta + g(\varphi)|\tan\theta|^3 \quad (1)$$

where $f_0 \equiv f(0,0)$ for a main crystalline plane, h is the step height, and $\beta(\varphi)$ and $g(\varphi)$ are the contributions of isolated steps and step interactions, respectively. When the heating temperature is elevated and/or the annealing time is increased, the thermodynamic function $f(\theta,\varphi)$ is minimized by changing the step height and/or the azimuth angle, leaving the miscutting angle constant. Therefore, rehabilitation of the substrate surface by annealing has another advantage, facilitating formation of large-scale terraces that could further improve the crystallinity of as-grown films depending on the annealing time and temperature.

Figure 1 shows the AFM images of (001) MgO substrates that are same as those used for deposition of the LBCO films. The as-received MgO substrate exhibits a smooth surface with a root-mean-square (rms) roughness of ∼0.25 nm measured in the 4 × 4 μm AFM image, as shown in Figure 1a, indicating the substrate was well-prepared. However, the high-frequency zigzag morphology makes the surface terraces invisible in the AFM image. In addition, some attachments are occasionally observed on the surface. After annealing at 1200 °C for 3 h, the substrate surface changed to be very clean, and terraces with wave-shaped edges appeared in the AFM image, as shown in Figure 1b. Though the rms roughness increased to ∼0.76 nm due to the appearance of terraces, the high-frequency zigzag morphology disappeared. More importantly, the terrace surface looks more solidified and much smoother than that of the as-received one, suggesting that defects on the surface were effectively removed. When the height profiles of scanning lines in the AFM images were quantitatively analyzed, the fluctuation in the height on the same terraces is determined to be within 0.1 nm, and the step height of the vicinal terraces varies from 0.5 to ∼3 nm, as shown in Figure S1, indicating that both the isolated steps and the step interaction terms in eq 1 contribute to the formation of the terrace morphology.[17] On the substrate annealed at 1350 °C, the terraces with the straight edges appeared and changed to the micrometer scale, in accordance with the theoretical predication. The surface height on the large-scale terraces fluctuates from 0.2 to ∼0.8 nm, suggesting new terraces along the edge direction developed. Therefore, the term of the step interactions in eq 1 starts to dominate the morphological evolution on these large-scale terraces.[17] On the other hand, quantitative analysis revealed that the steps between the large-scale vicinal terraces changed to be as high as ∼10 nm, as shown in Figure S1; thus, they could be regarded as the new crystallographic surfaces[17] dominating the further evolution of the surface morphology. On these terrace surfaces, we observed some small islands and attachments, which are probably the remains resulting from the evolution of morphology or due to pollution during the annealing process. Annealing the substrate at 1400 °C leads to a smooth surface with an rms roughness of ∼0.64 nm, but the flat terraces disappear. Instead, the substrate surface exhibits a typical morphology with a melting feature. At the same time, we observed as large as ∼100 nm holes and a large amount of pits, which can be attributed to the dislocations in the crystal. The small and white points might be due to pollution in the annealing process or the impurities in the crystal. The above AFM images definitely demonstrate that the thermal rehabilitation of the MgO substrate is more effective at temperatures below 1400 °C.

Deposition parameters, including the Ar:O_2 ratio, working pressure, RF power, and substrate temperature, were optimized to obtain highly epitaxial LBCO films.[15] We found that temperature and deposition rate are the two crucial factors in the growth of highly epitaxial LBCO films. In this study, the LBCO films were deposited at the optimized parameters of 830 °C, 80 W, and 4.5 Pa. AES analysis showed that La, Ba, Co, and O are the visible signals in the as-grown films, as shown in Figure S2, indicating that the impurity elements are lower than the detection limit (∼1 wt. %). The EDX spectra of the LBCO films are shown in Figure 2. As the signals of C, Si, and Mo were not detected by AES, we ascribed them to the impurity elements in the substrates. As indicted in the figure, Ba and La have highly overlapping EDX spectra, making quantitative analysis difficult. Under the assumption that Ba and La have the same sensitivity in the EDX spectra, we estimated the atomic ratio of La and Ba to Co to be close to 1:1.

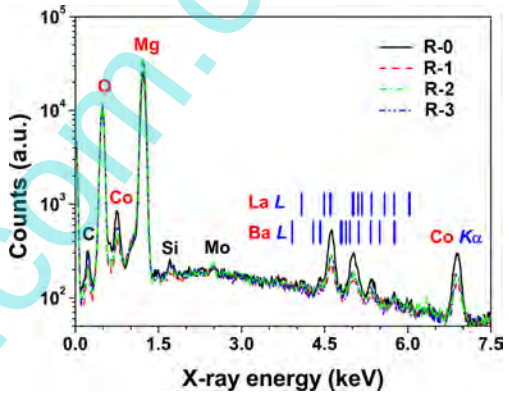

Figure 2. EDX spectra of the LBCO films grown on the MgO substrates in which C, Si, and Mo were attributed to the impurity elements in the substrates because they were undetected by AES.

The AFM morphology of the LBCO films grown on the as-received and rehabbed substrates is depicted in Figure 3. Compared with the AFM image of the film grown on the as-received substrate (R-0), those of the films grown on the annealed substrates (R-1, R-2, and R-3) exhibit the morphology with more solidified structures. The R-0 sample consists of∼50 nm grains, producing a 4.22 nm rms roughness in the 1 × 1 μm AFM image. In contrast with the R-0 sample, no obvious grain boundary could be observed on the surface morphology of the films grown on the rehabbed MgO substrates, as shown in Figures 3b−d, indicating they are closer to the single-crystal films. The single-crystal feature is further evidenced by the dome-shaped islands independently standing on the film surfaces, as shown in the AFM images, because such islands are known as surface ripples induced by strains caused by the mismatch between film and substrate[18] and are popularly observed in the growth of single-crystal films with a mismatch for the substrate. Furthermore, we found the difference in the AFM transverse-force images between the islands and the surrounded area is negligible (<0.04 V), as shown in Figure S3; thus, the compositions in the islands and films could be

DOI: 10.1021/acs.cgd.6b00308
Cryst. Growth Des. 2016, 16, 4272−4277

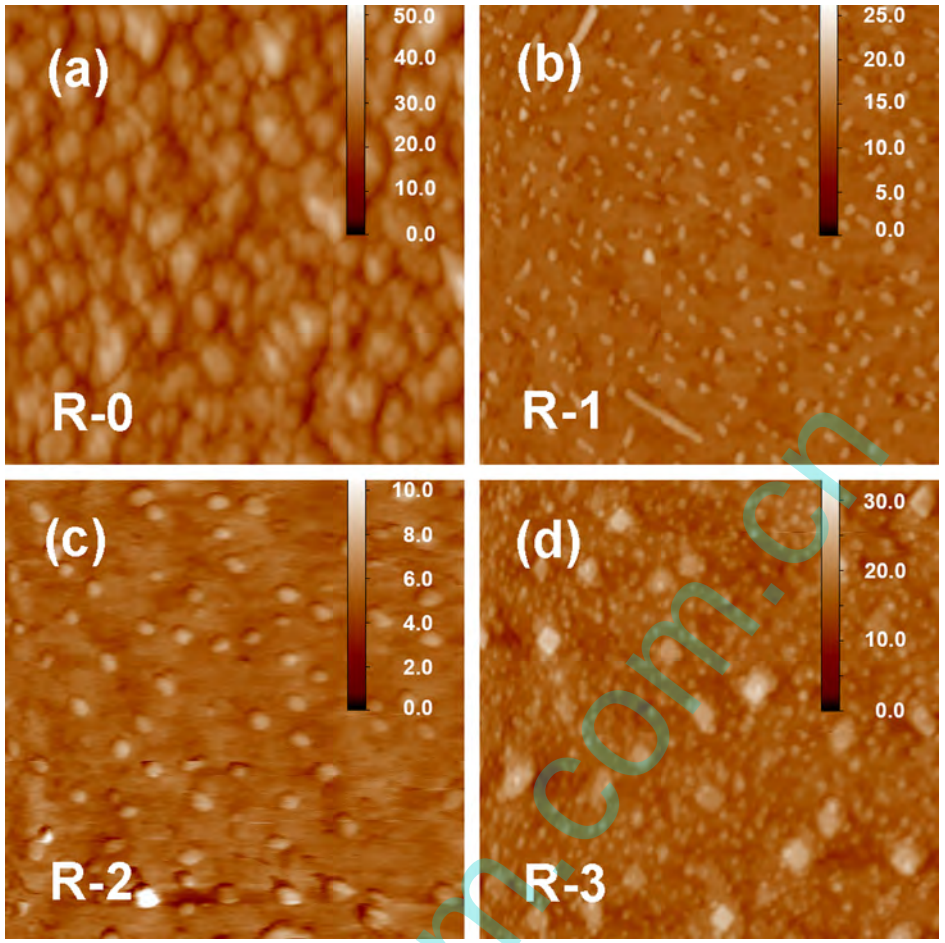

Figure 3. AFM images (1 × 1 μm) of the LBCO films grown on (a) the as-received substrate and (b–d) the substrates annealed at the temperatures of 1200, 1350, and 1400 °C, respectively. The color rules are in nanometers to represent the variation in height.

regarded as the same. On the other hand, these islands are lying in two specific directions, suggesting their dependence on the film lattices. When the annealing temperature of the substrate was elevated, the size of the surface islands increased, indicating that the film strains could be modulated by rehabbing substrate surface through changing the annealing temperature or annealing time. The rms roughness of R-1, R-2, and R-3 samples was measured to be 1.14, 0.67, and 2.25 nm, respectively, much lower than that of the film grown on the as-received substrate.

XRD analysis confirmed that all of the as-grown LBCO films are highly epitaxial with the relationship of LBCO(001) // MgO(001) and LBCO [100] // MgO [100], as shown in Figure S4. The R-0 sample exhibited the largest full width at the half-maximum (fwhm) of the XRD (002) rocking curve (2.17°). For the films grown on the substrates annealed at the elevated temperatures at 1200, 1350, and 1400 °C, the fwhm of the XRD (002) rocking curve was decreased to 1.99°, 1.88°, and 1.21°, respectively, supporting the improvement in crystallinity. Figure 4 depicts the high-resolution XRD pattern and the asymmetric reciprocal space maps (RSMs) at (204) diffraction of the R-0 sample in comparison with that of the R-2 sample. Compared with those of the R-0 sample, the R-2 sample exhibits much more intense and narrower XRD peaks. At the same time, the MgO(002) peak is sharper in the rehabbed substrate than that in the as-received one, evidencing the validity of substrate rehabilitation by annealing. Therefore, we have a confident conclusion that substrate annealing not only rehabbed the damaged lattices in a depth of layers beneath the MgO surface but also improved the as-grown LBCO film in crystallinity. The improvement in the substrate and the LBCO film is more accurately presented in the asymmetric RSMs, in which the substrate and the film exhibits the sharper XRD (204) peaks when the substrate is annealed at 1350 °C for 3 h. At the same time, the XRD intensity of MgO(002) from the strained zone of the rehabbed substrate is much lower than that of the as-received one, strongly supporting the validity of annealing rehabilitation.

Using the RSMs, the lattice parameters of the LBCO film in the R-2 sample were determined to be a = 0.3869 nm and c = 0.3908 nm, differing from those of R-0 (a = 0.3854 nm and c = 0.3901 nm). The rehabbed substrate produces an increase of ~1.0% in the unit cell of the LBCO film. Therefore, we could further deduce that rehabilitation of substrate surface by annealing is capable of modulating the lattice parameters of the as-grown films by changing the substrate surface morphology, such as the change in the terrace width and the step height. As a result, the physical properties of LBCO films could be changed by the substrate annealing process because perovskite oxides are the materials with properties sensitive to their lattice parameters.[19] As a matter of fact, the electrical transport properties of the as-grown LBCO films deposited by the PLD method have been found to be strongly dependent on the miscutting angles of substrates,[8,10] and the dependence is

DOI: 10.1021/acs.cgd.6b00308
Cryst. Growth Des. 2016, 16, 4272–4277

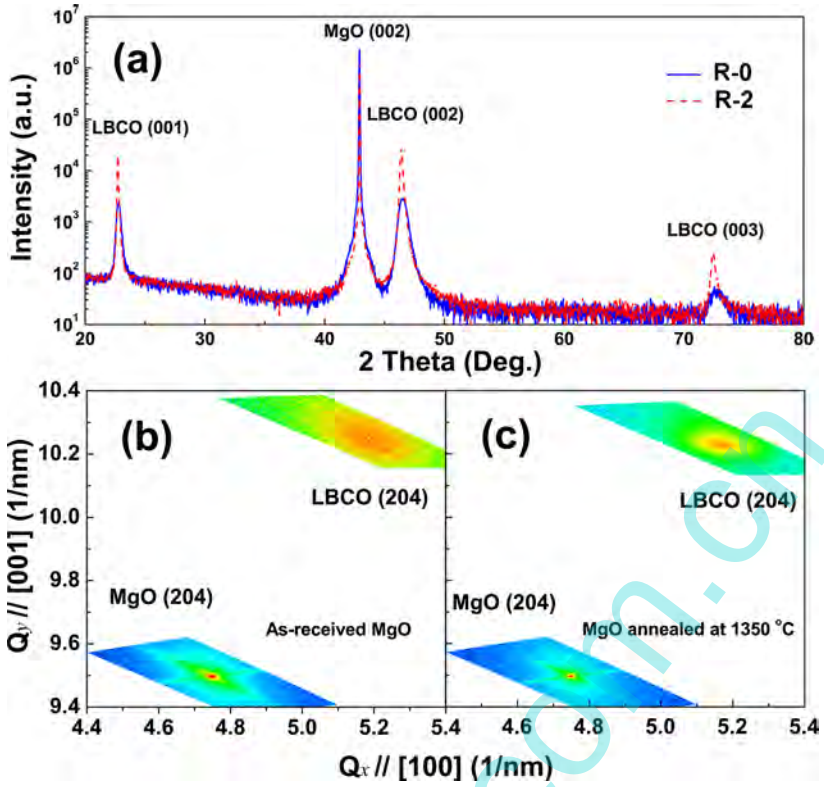

Figure 4. High-resolution XRD patterns and RSMs of R-0 and R-2 samples. The color in RSMs represents the XRD intensity varying in logarithmic scale, and the maximum scales for LBCO(204) and MgO(204) are 10^4 and 10^7 in counts, respectively.

attributed to the difference in the terrace width. In this study, we provide substrate annealing as an alternative method to tune the physical properties of the as-grown LBCO films. More importantly, substrate annealing is an effective method to improve the LBCO films in crystallinity, and solid evidence is presented to support the growth of the single-crystal LBCO films on the rehabbed (001) MgO substrate using the RF magnetron sputtering method, paving the way for cost-effective and large-scale applications. Furthermore, the principle demonstrated in this study could be applied to rehabilitate other substrates because surface damage is ubiquitous in manufacturing and surface milling; thus, the performance of the devices based on single-crystal films could be further improved when rehabilitation of substrate surface is applied. Therefore, we are convinced that rehabilitation of the substrate surface by annealing has potential for a range of applications, such as fabrication of light emitting diodes, optoelectronic detectors, and gas sensors.

4. CONCLUSIONS

In conclusion, we demonstrated the validity of substrate annealing for growth of high-quality epitaxial films. After being annealed at temperatures of 1200−1400 °C for 3 h, the damaged surfaces of (001) MgO substrates were rehabbed and thus more solidified, and single-crystal LBCO films were obtained using RF magnetron sputtering at optimized conditions. The improvement of the crystallinity of LBCO films is essentially attributed to the rehabilitation of the damaged substrate surface induced by manufacturing and surface milling. The principle for rehabbing the damaged surfaces of epitaxial substrates could be applied to improve the performance of devices based on single-crystal films and has the potential for application in a number of advanced technologies related to microelectronics, optoelectronics, spintronics, and superconducting electronics.

■ ASSOCIATED CONTENT

Supporting Information

The Supporting Information is available free of charge on the ACS Publications website at DOI: 10.1021/acs.cgd.6b00308.

Height profiles of the rehabbed MgO surface, AES spectrum of the LBCO film, AFM transverse-force image of the LBCO film, and $\theta-2\theta$ and φ-scan XRD patterns of LBCO films (PDF)

■ AUTHOR INFORMATION

Corresponding Author

*E-mail: qyzhang@dlut.edu.cn.

Notes

The authors declare no competing financial interest.

■ ACKNOWLEDGMENTS

J.S. would like to thank the support of the Chinese Government Scholarship (Grant 2012736005). The research at Xi'an Jiaotong University was financially supported by the National Natural Science Foundation of China under Grant 51202185.

■ REFERENCES

(1) Rautama, E. L.; Boullay, P.; Kundu, A. K.; Caignaert, V.; Pralong, V.; Karppinen, M.; Raveau, B. Cationic Ordering and Microstructural Effects in the Ferromagnetic Perovskite $La_{0.5}Ba_{0.5}CoO_3$: Impact upon Magnetotransport Properties. *Chem. Mater.* **2008**, *20*, 2742.

(2) Ishihara, T.; Fukui, S.; Nishiguchi, H.; Takita, Y. Mixed electronic-oxide ionic conductor of $BaCoO_3$ doped with La for

DOI: 10.1021/acs.cgd.6b00308
Cryst. Growth Des. 2016, 16, 4272−4277

cathode of intermediate-temperature- operating solid oxide fuel cell. *Solid State Ionics* **2002**, *152−153*, 609.
(3) Setevich, C.; Mogni, L.; Caneiro, A.; Prado, F. Characterization of the $La_{1-x}Ba_xCoO_{3-\delta}$ ($0 \leq x \leq 1$) System as Cathode Material for IT-SOFC. *J. Electrochem. Soc.* **2012**, *159*, B73.
(4) Pang, S. L.; Jiang, X. N.; Li, X. N.; Wang, Q.; Zhang, Q. Y. Structural stability and high-temperature electrical properties of cation-ordered/disordered perovskite LaBaCoO. *Mater. Chem. Phys.* **2012**, *131*, 642.
(5) Pang, S.L.; Jiang, X. N.; Li, X. N.; Xu, H. X.; Jiang, L.; Xu, Q. L.; Shi, Y. C.; Zhang, Q. Y. Structure and properties of layered-perovskite $LaBa_{1-x}Co_2O_{5+\delta}$ (x = 0−0.15) as intermediate-temperature cathode material. *J. Power Sources* **2013**, *240*, 54.
(6) Liu, M.; Liu, J.; Collins, G.; Ma, C. R.; Chen, C. L.; He, J.; Jiang, J. C.; Meletis, E. I.; Jacobson, A. J.; Zhang, Q. Y. Magnetic and transport properties of epitaxial $(LaBa)Co_2O_{5.5+\delta}$ thin films on(001) $SrTiO_3$. *Appl. Phys. Lett.* **2010**, *96*, 132106.
(7) Liu, M.; Ma, C. R.; Liu, J.; Collins, G.; Chen, C. L.; He, J.; Jiang, J. C.; Meletis, E. I.; Sun, L.; Jacobson, A. J.; Whangbo, M.-H. Giant Magnetoresistance and Anomalous Magnetic Properties of Highly Epitaxial Ferromagnetic $LaBaCo_2O_{5.5+\delta}$ Thin Films on (001) MgO. *ACS Appl. Mater. Interfaces* **2012**, *4*, 5524.
(8) Ma, C. R.; Liu, M.; Collins, G.; Wang, H. B.; Bao, S. Y.; Xu, X.; Enriquez, E.; Chen, C. L.; Lin, Y.; Whangbo, M.-H. Magnetic and Electrical Transport Properties of $LaBaCo_2O_{5.5+\delta}$ Thin Films on Vicinal (001) $SrTiO_3$ Surfaces. *ACS Appl. Mater. Interfaces* **2013**, *5*, 451.
(9) Ma, C. R.; Liu, M.; Liu, J.; Collins, G.; Zhang, Y. M.; Wang, H. B.; Chen, C. L.; Lin, Y.; He, J.; Jiang, J. C.; Meletis, E. I.; Jacobson, A. J. Interface Effects on the Electronic Transport Properties in Highly Epitaxial $LaBaCo_2O_{5.5+\delta}$ Films. *ACS Appl. Mater. Interfaces* **2014**, *6*, 2540.
(10) Zou, Q.; Liu, M.; Wang, G. Q.; Lu, H. L.; Yang, T. Z.; Guo, H. M.; Ma, C. R.; Xu, X.; Zhang, M. H.; Jiang, J. C.; Meletis, E. I.; Lin, Y.; Gao, H. J.; Chen, C. L. Step Terrace Tuned Anisotropic Transport Properties of Highly Epitaxial $LaBaCo_2O_{5.5+\delta}$ Thin Films on Vicinal SrTiO3 Substrates. *ACS Appl. Mater. Interfaces* **2014**, *6*, 6704.
(11) Liu, M.; Zou, Q.; Ma, C. R.; Collins, G.; Mi, S. B.; Jia, C. L.; Guo, H. M.; Gao, H. J.; Chen, C. L. Strain-Induced Anisotropic Transport Properties of $LaBaCo_2O_{5.5+\delta}$Thin Films on $NdGaO_3$ Substrates. *ACS Appl. Mater. Interfaces* **2014**, *6*, 8526.
(12) Liu, J.; Collins, G.; Liu, M.; Chen, C. L.; Jiang, J. C.; Meletis, E. I.; Zhang, Q. Y.; Dong, C. PO2 dependant resistance switch effect in highly epitaxial $(LaBa)Co_2O_{5.5+\delta}$ thin films. *Appl. Phys. Lett.* **2010**, *97*, 094101.
(13) Bao, S. Y.; Ma, C. R.; Chen, G.; Xu, X.; Enriquez, E.; Chen, C. L.; Zhang, Y. M.; Bettis, J. L.; Whangbo, M.-H.; Dong, C.; Zhang, Q. Y. Ultrafast Atomic Layer- by-Layer OxygenVacancy-Exchange Diffusion in Double-Perovskite $LnBaCo_2O_{5.5+\delta}$ Thin Films. *Sci. Rep.* **2014**, *4*, 4726.
(14) Liu, M.; Ren, S. P.; Zhang, R. Y.; Xue, Z. Y.; Ma, C. R.; Yin, M. L.; Xu, X.; Bao, S. Y.; Chen, C. L. Gas Sensing Properties of Epitaxial $LaBaCo_2O_{5.5+\delta}$ Thin Films. *Sci. Rep.* **2015**, *5*, 10784.
(15) Ju, J. Dalian University of Technology, Influence of substrate annealing on the growth of LBCO films. PhD. thesis, 2013.
(16) Millange, F.; Caignaert, V.; Domenges, B.; Raveau, B.; Suard, E. Order-Disorder Phenomena in New LaBaMn2O6-x CMR Perovskites. Crystal and Magnetic Structure. *Chem. Mater.* **1998**, *10*, 1974.
(17) Kurnosikov, O.; Pham Van, L.; Cousty, J. About anisotropy of atomic-scale height step on (0001) sapphire surface. *Surf. Sci.* **2000**, *459*, 256.
(18) Ohring, M. *Materials Science of Thin films−Deposition and Structure*; Academic Press: Cambridge, MA, 2002; p 434.
(19) Millis, A. J. Lattice effects in magnetoresistive manganese perovskites. *Nature* **1998**, *392*, 147.

DOI: 10.1021/acs.cgd.6b00308
Cryst. Growth Des. 2016, 16, 4272−4277